

EFFECTS OF HEAT SOURCE/SINK ON DARCIAN-BÈNARD-MAGNETO-MARANGONI CONVECTIVE INSTABILITY IN A COMPOSITE LAYER SUBJECTED TO NONUNIFORM TEMPERATURE GRADIENTS

N. MANJUNATHA¹, R. SUMITHRA², §

ABSTRACT. The problem of Bènard-Magneto-Marangoni convection in a composite layer which is infinite along x and y directions is considered for the Darcian case in the presence of constant heat source/sink in both the layers. This composite layer is subjected to uniform and nonuniform temperature gradients. The eigenvalue, thermal Marangoni number is obtained in closed form with the lower surface rigid and upper surface free with surface tension effects for the velocity and isothermal temperature boundary combinations. The influence of porous parameter, magnetic field and nonuniform temperature gradients on the Eigen value problem are discussed. It is experiential that the effect of heat source/sink in the fluid layer is dominant on the eigenvalue over the same in the porous layer. The important parameters like Chandrasekhar number, modified internal Rayleigh number and thermal ratio which control Bènard-Magneto-Marangoni convection are discussed in detail.

Keywords: Heat source (sink), Bènard-Magneto-Marangoni convection, Exact method, Depth ratio, Temperature gradients, Isothermal boundaries.

AMS Subject Classification: 80-XX, 80Axx, 80A20.

1. INTRODUCTION

The hydro-magnetic fluid flow problems combined with the effects of the heat transport phenomenon in a porous system are one of the useful problems in the field of fluid engineering because of their rheological implication and applied germaneness. Sheeting stuff (paper, fiber and metallic sheets), glass blowing and manufacturing, casting and coating of wires, synthetic fiber, purification of molten metals from a nonmetallic inclusion due to magnetic field application, crystal growing, etc. Recently, various applied mathematicians and researchers have proposed that the cooling rate is critical for the products to enhance their quality. The study of the effect of the magnetic field on temperature distribution with heat source/sink when fluid is capable of emitting and absorbing thermal radiations

¹ School of Applied Sciences, REVA University, Bengaluru, Karnataka, India.

e-mail: manjunatha.n@reva.edu.in; ORCID: <https://orcid.org/0000-0002-7076-7122>.

² Department of UG, PG Studies & Research in Mathematics, Nrupathunga University, Bengaluru, Karnataka, India.

e-mail: sumitra-diya@yahoo.com; ORCID: <https://orcid.org/0000-0003-2199-1918>.

§ Manuscript received: May 15, 2020; accepted: August 14, 2020.

TWMS Journal of Applied and Engineering Mathematics, Vol.12, No.3 © Işık University, Department of Mathematics, 2022; all rights reserved.

is of great importance in concerned with space applications and higher operating temperatures. The study of heat generation or absorption in moving fluids is important in several physical problems such as fluids undergoing exothermic or endothermic chemical reactions. The effect of heat source/sink in thermal convection is considered where there are high-temperature differences between surfaces such as spacecraft bodies. The study of heat source/sink effects on heat transfer is very important because their effects are crucial in controlling the heat transfer also used as an effective parameter to control convection. The natural convection process in the presence of a heat source/sink is presented in various physical phenomena such as fire engineering, combustion modeling, nuclear energy, heat exchangers, petroleum reservoir, etc. Internal heat source (sink) may arise due to heat released during chemical reactions in the fluid, radioactive decay, Ohmic heating by the current in a conductive liquid, produced by radiation from the external medium thereby helping in advancing or delaying convection. The several studies have been made on the single layer, Sankar *et al.* [1, 2, 3] examined the effect of the magnetic field on natural convection in a vertical cylindrical and the porous annulus in the presence of an internal heat source. Swati Mukhopadhyay [4] studied the steady natural convection boundary-layer flow in the neighbourhood of lower stagnation point of a heated sphere embedded in a saturated porous medium in the presence of a heat source/sink using shooting technique. Mixed convection flow of conducting fluid in a vertical channel with boundary conditions of the third kind in the presence of heat source/sink studied by Umavathi *et al.* [5]. Brian Straughan [6] studied the linear instability and nonlinear stability analysis of the situation of convection in a horizontal plane layer of fluid when there is a heat sink/source which is linear in the vertical coordinate which is in the opposite direction of gravity. The effect of mass transfer on unsteady hydromagnetic convective flow, of an incompressible electrically conducting fluid, past an infinite vertical rotating porous plate in the presence of constant injection and heat source has been investigated by Thomas Mwathi Ngugi *et al.* [7]. Malvandi *et al.* [8] investigated the effect of thermal asymmetry on forced convection of alumina/water nanofluid in a parallel-plate microchannel in the presence of a heat source/sink is theoretically. Baag *et al.* [9] studied the effects of mass buoyancy, uniform heat source/sink and first order chemical reaction using the shooting technique with the help of the Runge-Kutta method of fourth order. Umavathi *et al.* [10] studied the flow and heat transfer of couple stress fluid in a vertical channel in the presence of heat source/sink analytically by the differential transform method and numerically by the Runge-Kutta shooting method. Singh and Singh [11] studied the effect of the heat source/sink parameter on the free convective flow of a polar fluid in open-ended vertical concentric annuli. Ganesh Kumar *et al.* [12] examined the impact of the convective condition on Marangoni convection in Casson nanofluid with including the uniform heat source/sink using the RKF-45 method. Anjali Devi *et al.* [13] analyzed the effects of radiation on an MHD boundary layer flow and heat transfer over a nonlinear stretching surface with variable wall temperature and non-uniform heat source/sink using the Nachtsheim Swigert shooting iteration technique together with the fourth order Runge Kutta method. Ramachandramurthy and Aruna [14] deals with linear stability analysis of Rayleigh-Bènard convection in a rotating Newtonian fluid with heat source/sink confined between two parallel, infinitely extended horizontal surfaces. Using the Laplace transformation technique, the effect of heat source or sink past an impulsively started vertical and infinite vertical plate under the influence of the transverse magnetic field has been investigated by Garg and Shipra [15, 16, 17]. They obtained the exact solution to the problem. Shipra and Garg [18] studied the effects of heat source/sink and chemical reaction with mass diffusion on free convective incompressible viscous fluid flow past an

accelerated vertical plate with a magnetic field. They have used the Laplace transform method to solve the system of linear partial differential equations. Girish *et al.* [19, 20] deliberated numerically as well as analytically the fully developed mixed convective flow in the vertical annuli having two annular passages with open upper and lower boundaries by considering viscous dissipation also imposing unheated entry and unheated exit thermal boundary conditions. Naveen Dwivedi and Singh [21] studied the fully developed laminar magnetohydrodynamic free convection between two concentric vertical cylinders with hall currents and heat source/sink, in the presence of the radial magnetic field. They found that the influence of the hall parameter enhances the velocity fields in the appearance of heat source and sink. Mebarek-Oudina *et al.* [22] deliberates the impacts of the location of a thermal source of buoyant convection of nanofluids in an annular region are analyzed numerically through the finite volume technique. Five different thermal source positions along the inner cylinder of the annulus have been analyzed.

For the composite layers, Sumithra and Manjunatha [23, 24, 25] considered the effect of non-uniform temperature gradients on single and double-diffusive magneto-Marangoni convection in a two-layer system and also in the presence of constant heat source. Sumithra *et al.* [26] studied the effects of heat source/sink and non-uniform temperature gradients on non-Darcian-Benard-Magneto-Marangoni convection in an infinite horizontal composite layer. They obtained the closed-form of solution for three different thermal Marangoni numbers.

So far no attempt has been made to analyze the effects in a composite layer with constant heat source/sink and uniform and non-uniform temperature gradients in the presence of a magnetic field and hence the present work is focused on this. In the present paper, an attempt is made to study the effect of non-uniform temperature gradients on Darcy-Bénard-Magneto-Marangoni convection in a composite layer in the presence of a constant heat source (sink) in both the layers.

2. MATHEMATICAL FORMULATION

The composite layer system under investigation is shown in Figure 1. Consider a horizontal single component, electrically conducting fluid saturated isotropic densely packed porous layer of thickness d_m underlying a single component fluid layer of thickness d with an imposed magnetic field intensity H_0 in the vertical Z -direction and with heat sources Φ_m and Φ respectively. The lower isothermal surface of the porous layer rigid and the upper isothermal surface of the fluid layer is free with surface tension effects depending on temperature. A Cartesian coordinate system is chosen with the origin at the interface between porous and fluid layers and the Z -axis, vertically upwards.

The basic equations for fluid and porous layer respectively governing such a system are,

$$\nabla \cdot \vec{q} = 0 \tag{1}$$

$$\nabla \cdot \vec{H} = 0 \tag{2}$$

$$\rho_0 \left[\frac{\partial \vec{q}}{\partial t} + (\vec{q} \cdot \nabla) \vec{q} \right] = -\nabla P + \mu \nabla^2 \vec{q} + \mu_p (\vec{H} \cdot \nabla) \vec{H} \tag{3}$$

$$\frac{\partial T}{\partial t} + (\vec{q} \cdot \nabla) T = \kappa \nabla^2 T + \Phi \tag{4}$$

$$\frac{\partial \vec{H}}{\partial t} = \nabla \times \vec{q} \times \vec{H} + \nu_m \nabla^2 \vec{H} \tag{5}$$

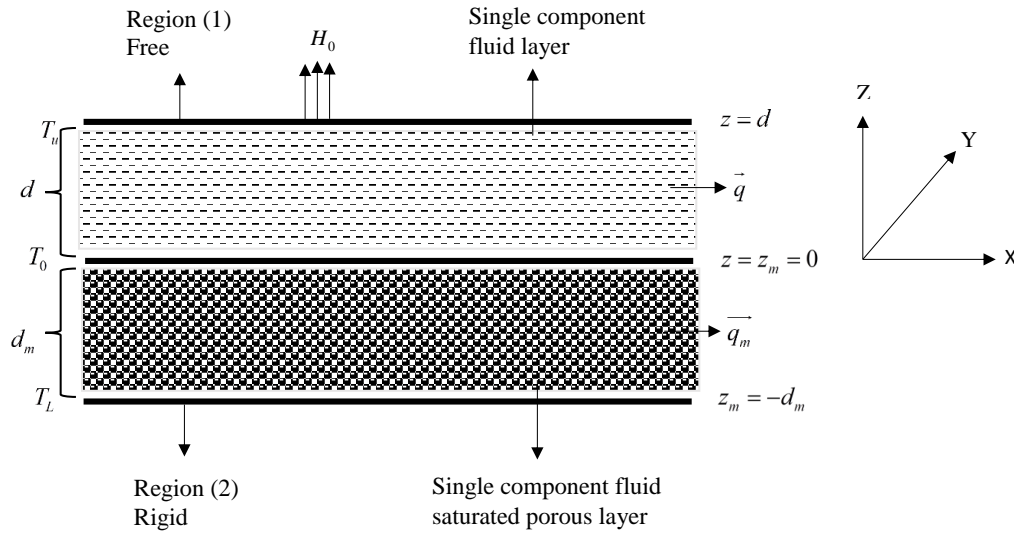


FIGURE 1. Geometry of the problem

$$\nabla_m \cdot \vec{q}_m = 0 \tag{6}$$

$$\nabla_m \cdot \vec{H} = 0 \tag{7}$$

$$\rho_0 \left[\frac{1}{\varepsilon} \frac{\partial \vec{q}_m}{\partial t} + \frac{1}{\varepsilon^2} (\vec{q}_m \cdot \nabla_m) \vec{q}_m \right] = -\nabla_m P_m - \frac{\mu}{K} \vec{q}_m + \mu_p (\vec{H} \cdot \nabla_m) \vec{H} \tag{8}$$

$$A \frac{\partial T_m}{\partial t} + (\vec{q}_m \cdot \nabla_m) T_m = \kappa_m \nabla_m^2 T_m + \Phi_m \tag{9}$$

$$\varepsilon \frac{\partial \vec{H}}{\partial t} = \nabla_m \times \vec{q}_m \times \vec{H} + \nu_{em} \nabla_m^2 \vec{H} \tag{10}$$

where, for fluid layer, \vec{q} is the velocity vector, ρ_0 is the fluid density, t is the time, μ is the fluid viscosity, $P = p + \frac{\mu_p H^2}{2}$ is the total pressure, \vec{H} is the magnetic field, T is the temperature, κ is the thermal diffusivity of the fluid, $\nu_m = \frac{1}{\mu_p \sigma}$ is the magnetic viscosity and μ_p is the magnetic permeability. For porous layer ε is the porosity, μ is the fluid viscosity of the porous layer, K is the permeability of the porous medium, A is the ratio of heat capacities, κ_m is the thermal diffusivity, $\nu_{em} = \frac{\nu_m}{\varepsilon}$ is the effective magnetic viscosity and the subscript 'm' denotes the quantities in porous layer.

The aim of this paper is to investigate the stability of infinitesimal perturbations superposed on the basic quiescent state. The basic state of the liquid being quiescent is described by

$$\vec{q} = \vec{q}_b = 0, P = P_b(z), T = T_b(z), \vec{H} = H_0(z) \tag{11}$$

$$\vec{q}_m = \vec{q}_{mb}, P_m = P_{mb}(z_m), T_m = T_{mb}(z_m), \vec{H} = H_0(z_m) \tag{12}$$

The basic state temperatures of $T_b(z)$ and $T_{mb}(z_m)$ are obtained as

$$T_b(z) = \frac{-\Phi z(z-d)}{2\kappa} + \frac{(T_u - T_0)h(z)}{d} + T_0 \quad 0 \leq z \leq d \tag{13}$$

$$T_{mb}(z_m) = \frac{-\Phi_m z_m(z_m + d_m)}{2\kappa_m} + \frac{(T_0 - T_l)h_m(z_m)}{d_m} + T_0 \quad -d_m \leq z_m \leq 0 \tag{14}$$

where $T_0 = \frac{\kappa d_m T_u + \kappa_m d T_l}{\kappa d_m + \kappa_m d} + \frac{d d_m (\Phi_m d_m + \Phi d)}{2(\kappa d_m + \kappa_m d)}$ is the interface temperature, $h(z)$ & $h_m(z_m)$ are the nondimensional temperature gradients in fluid and porous layer respectively and subscript 'b' denote the basic state.

We superimpose infinitesimal disturbances on the basic state for fluid and porous layer respectively

$$\vec{q} = \vec{q}_b + \vec{q}', P = P_b + P', T = T_b(z) + \theta, \vec{H} = H_0(z) + \vec{H}' \tag{15}$$

$$\vec{q}_m = \vec{q}_{mb} + \vec{q}_m', P_m = P_{mb} + P_m', T_m = T_{mb}(z_m) + \theta_m, \vec{H} = H_0(z_m) + \vec{H}' \tag{16}$$

where the prime indicates the perturbations. Introducing (15) and (16) in (1) - (10), operating curl twice and eliminate the pressure term from equations (3) and (8). The variables are then nondimensionalised using $d, \frac{d^2}{\kappa}, \frac{\kappa}{d}, T_0 - T_u$ and H_0 as the units of length, time, velocity, temperature and the magnetic field in the fluid layer and $d_m, \frac{d_m^2}{\kappa_m}, \frac{\kappa_m}{d_m}, T_l - T_0$ as the corresponding characteristic quantities in the porous layer.

The dimensionless equations are then subjected to normal mode analysis as follows

$$\begin{bmatrix} W \\ \theta \\ H \end{bmatrix} = \begin{bmatrix} W(z) \\ \theta(z) \\ H(z) \end{bmatrix} f(x, y) e^{nt} \tag{17}$$

$$\begin{bmatrix} W_m \\ \theta_m \\ H \end{bmatrix} = \begin{bmatrix} W_m(z_m) \\ \theta_m(z_m) \\ H(z_m) \end{bmatrix} f_m(x_m, y_m) e^{n_m t} \tag{18}$$

with $\nabla_2^2 f + a^2 f = 0$ and $\nabla_{2m}^2 f_m + a_m^2 f_m = 0$, where a and a_m are the horizontal wave numbers, n and n_m are the frequencies, W & W_m are the dimensionless vertical velocities, θ & θ_m are temperature distributions in fluid and porous layer respectively and obtain the following equations

in $0 \leq z \leq 1$

$$(D^2 - a^2 + \frac{n}{Pr})(D^2 - a^2)W = -Q\tau_{fm}D(D^2 - a^2)H \tag{19}$$

$$(D^2 - a^2 + n)\theta + [h(z) + R_f^*(2z - 1)]W = 0 \tag{20}$$

$$(\tau_{fm}(D^2 - a^2) + n)H + DW = 0 \tag{21}$$

in $-1 \leq z_m \leq 0$

$$(1 - \frac{\beta^2 n_m}{Pr_m})(D_m^2 - a_m^2)W_m = Q_m \tau_{mm} \beta^2 D_m (D_m^2 - a_m^2)H_m \tag{22}$$

$$(D_m^2 - a_m^2 + An_m)\theta_m + [h_m(z_m) + R_m^*(2z_m + 1)]W_m = 0 \tag{23}$$

$$(\tau_{mm}(D_m^2 - a_m^2) + n_m \varepsilon)H_m + D_m W_m = 0 \tag{24}$$

where, for fluid layer $Pr = \frac{\nu}{\kappa}$ is the Prandtl number, $Q = \frac{\mu_p H_0^2 d^2}{\mu \kappa \tau_{fm}}$ is the Chandrasekhar number and $\tau_{fm} = \frac{\nu_{mv}}{\kappa}$ is the diffusivity ratio. For porous layer, $Pr_m = \frac{\varepsilon \nu_m}{\kappa_m}$ is the Prandtl number, $\beta^2 = \frac{K}{d_m^2} = Da$ is the Darcy number, β is the porous parameter, $Q_m = \frac{\mu_p H_0^2 d_m^2}{\mu \kappa_m \tau_{mm}} = Q \varepsilon \hat{d}^2$ is the Chandrasekhar number and $\tau_{mm} = \frac{\nu_{em}}{\kappa_m}$ is the diffusivity ratio of fluid in porous layer. $R_I^* = \frac{R_I}{2(T_0 - T_u)}$ and $R_{Im}^* = \frac{R_{Im}}{2(T_l - T_0)}$ are the modified internal Rayleigh numbers for fluid and porous layer and $R_I = \frac{\Phi d^2}{\kappa}$ and $R_{Im} = \frac{\Phi_m d_m^2}{\kappa_m}$ are the internal Rayleigh numbers for fluid and porous layer respectively. Substituting (21) in (19) & (24) in (22) and assume that the present problem satisfies the principle of exchange of stability, so putting $n = n_m = 0$. Now (19)-(24) becomes, in $0 \leq z \leq 1$

$$(D^2 - a^2)^2 W = Q D^2 W \tag{25}$$

$$(D^2 - a^2)\theta + [h(z) + R_I^*(2z - 1)]W = 0 \tag{26}$$

in $-1 \leq z_m \leq 0$

$$(D_m^2 - a_m^2)W_m = -Q_m \beta^2 D_m^2 W_m \tag{27}$$

$$(D_m^2 - a_m^2)\theta_m + [h_m(z_m) + R_{Im}^*(2z_m + 1)]W_m = 0 \tag{28}$$

where $R_I^* = \frac{R_I}{2(T_0 - T_u)}$ and $R_{Im}^* = \frac{R_{Im}}{2(T_l - T_0)}$ are the modified internal Rayleigh numbers for fluid and porous layer respectively.

3. BOUNDARY CONDITIONS

The boundary conditions are nondimensionalized and then subjected to normal mode expansion and are

$$\begin{aligned} D^2 W(1) + M a^2 \theta(1) &= 0, \\ W(1) = 0, W_m(-1) = 0, \hat{T} W(0) &= W_m(0), \\ \hat{T} \hat{d} DW(0) &= D_m W_m(0), \\ \hat{T} \hat{d}^3 \beta^2 (D^3 W(0) - 3a^2 DW(0)) &= -D_m W_m(0), \\ \theta(1) = 0, \theta(0) &= \hat{T} \theta_m(0), \\ D\theta(0) = D_m \theta_m(0), \theta_m(-1) &= 0 \end{aligned} \tag{29}$$

where $\hat{T} = \frac{T_l - T_0}{T_0 - T_u}$ is the thermal ratio, $M = -\frac{\partial \sigma_t (T_0 - T_u) d}{\partial T \mu \kappa}$ is the thermal Marangoni number, $\beta = \sqrt{\frac{K}{d_m^2}}$ is the porous parameter and $\hat{d} = \frac{d_m}{d}$ is the depth ratio.

4. METHOD OF SOLUTION

The solutions W and W_m are obtained by solving (25) and (27) using the velocity boundary conditions of (29), we get

$$W(z) = A_1[\cosh \delta z + a_1 \sinh \delta z + a_2 \cosh \zeta z + a_3 \sinh \zeta z] \tag{30}$$

$$W_m(z_m) = A_1[a_4 \cosh \delta_m z_m + a_5 \sinh \delta_m z_m] \tag{31}$$

where

$$\begin{aligned} \delta &= \frac{\sqrt{Q} - \sqrt{Q + 4a^2}}{2}, \zeta = \frac{\sqrt{Q} + \sqrt{Q + 4a^2}}{2}, \delta_m = \sqrt{\frac{a_m^2}{1 + Q_m \beta^2}} \\ a_1 &= -\frac{\Delta_2 a_3}{\Delta_1}, a_2 = \frac{\Delta_5 \Delta_7 - \Delta_8 \Delta_4}{\Delta_3 \Delta_7 - \Delta_6 \Delta_4}, a_3 = \frac{\Delta_5 \Delta_6 - \Delta_8 \Delta_3}{\Delta_4 \Delta_6 - \Delta_7 \Delta_3}, \\ a_4 &= \widehat{T}(1 + a_2), a_5 = \frac{1}{\delta_m}(\widehat{T} \widehat{d} a_1 \delta + a_3 \zeta) \quad \Delta_1 = \widehat{d}^2 \beta^2 (\delta^3 - 3a^2 \delta) + \delta, \\ \Delta_2 &= \widehat{d}^2 \beta^2 (\zeta^3 - 3a^2 \zeta) + \zeta, \Delta_3 = \widehat{T} \cosh \delta_m, \\ \Delta_4 &= -\frac{\widehat{d} \widehat{T} \sinh \delta_m}{\delta_m} \left(\zeta - \frac{\Delta_2 \delta}{\Delta_1} \right), \Delta_5 = -\Delta_3, \\ \Delta_6 &= \cosh \zeta, \Delta_7 = \sinh \zeta - \left(\frac{\Delta_2}{\Delta_1} \right) \sinh \delta, \Delta_8 = -\cosh \delta \end{aligned}$$

4.1. **Linear temperature profile.** Consider the linear profile

$$h(z) = 1 \quad \text{and} \quad h_m(z_m) = 1 \tag{32}$$

substituting equation (32) into (26) and (28), the temperature distributions θ and θ_m are obtained using the temperature boundary conditions, as follows

$$\theta(z) = A_1[c_1 \cosh az + c_2 \sinh az + g_1(z)] \tag{33}$$

$$\theta_m(z_m) = A_1[c_3 \cosh a_m z_m + c_4 \sinh a_m z_m + g_{m1}(z_m)] \tag{34}$$

where

$$\begin{aligned} g_1(z) &= A_1[\delta_1 - \delta_2 + \delta_3 - \delta_4], g_{m1}(z_m) = A_1[\delta_5 - \delta_6] \\ \delta_1 &= \frac{(E_2 z + E_1)}{(\delta^2 - a^2)} (\cosh \delta z + a_1 \sinh \delta z) \\ \delta_2 &= \frac{2\delta E_2}{(\delta^2 - a^2)^2} (a_1 \cosh \delta z + \sinh \delta z) \\ \delta_3 &= \frac{(E_2 z + E_1)}{(\zeta^2 - a^2)} (a_2 \cosh \zeta z + a_3 \sinh \zeta z) \\ \delta_4 &= \frac{2\zeta E_2}{(\zeta^2 - a^2)^2} (a_3 \cosh \zeta z + a_2 \sinh \zeta z) \\ \delta_5 &= \frac{(E_{1m} + E_{2m} z_m)}{(\delta_m^2 - a_m^2)} (a_4 \cosh \delta_m z_m + a_5 \sinh \delta_m z_m) \\ \delta_6 &= \frac{2E_{2m} \delta_m}{(\delta_m^2 - a_m^2)^2} (a_5 \cosh \delta_m z_m + a_4 \sinh \delta_m z_m) \\ E_1 &= R_I^* - 1, E_2 = -2R_I^*, E_{1m} = -(R_{Im}^* + 1), E_{2m} = -2R_{Im}^* \\ c_1 &= c_3 \widehat{T} + \Delta_{10} - \Delta_{11}, c_2 = \frac{1}{a}(c_4 a_m + \Delta_{12} - \Delta_{13}), \\ c_3 &= \frac{\Delta_{16} \Delta_{18} + \Delta_{19} \Delta_{15}}{\Delta_{15} \Delta_{17} + \Delta_{18} \Delta_{14}}, c_4 = \frac{\Delta_{19} \Delta_{14} - \Delta_{16} \Delta_{17}}{\Delta_{18} \Delta_{14} + \Delta_{17} \Delta_{15}}, \\ \Delta_9 &= -[\delta_7 - \delta_8 + \delta_9 - \delta_{10}], \\ \delta_7 &= \frac{(E_2 + E_1)}{(\delta^2 - a^2)} (\cosh \delta + a_1 \sinh \delta), \end{aligned}$$

$$\begin{aligned} \delta_8 &= \left[\frac{2\delta E_2}{(\delta^2 - a^2)^2} \right] (a_1 \cosh \delta + \sinh \delta), \\ \delta_9 &= \frac{(E_2 + E_1)}{(\zeta^2 - a^2)} (a_2 \cosh \zeta + a_3 \sinh \zeta), \\ \delta_{10} &= \left[\frac{2\zeta E_2}{(\zeta^2 - a^2)^2} \right] (a_3 \cosh \zeta + a_2 \sinh \zeta), \\ \Delta_{10} &= \widehat{T} \left[\frac{E_{1m} a_4}{(\delta_m^2 - a_m^2)} - \frac{2E_{2m} \delta_m a_5}{(\delta_m^2 - a_m^2)^2} \right], \\ \Delta_{11} &= \frac{E_1}{(\delta^2 - a^2)} - \frac{2\delta a_1 E_2}{(\delta^2 - a^2)^2} + \frac{a_2 E_1}{(\zeta^2 - a^2)} - \frac{2\zeta a_3 E_2}{(\zeta^2 - a^2)^2}, \\ \Delta_{12} &= \left[\frac{E_{2m}}{(\delta_m^2 - a_m^2)} - \frac{2\delta_m^2 E_{2m}}{(\delta_m^2 - a_m^2)^2} \right] a_4 + \frac{a_5 E_{1m}}{(\delta_m^2 - a_m^2)} \\ \Delta_{13} &= \frac{E_1 \delta a_1 + E_2}{(\delta^2 - a^2)} - \frac{2E_2 \delta^2}{(\delta^2 - a^2)^2} + \frac{E_1 \zeta a_3 + E_2 a_2}{(\zeta^2 - a^2)} - \frac{2a_2 E_2 \zeta^2}{(\zeta^2 - a^2)^2}, \\ \Delta_{14} &= \cosh a_m, \Delta_{15} = \sinh a_m, \\ \Delta_{16} &= -\frac{E_{1m} - E_{2m}}{(\delta_m^2 - a_m^2)} (a_4 \cosh \delta_m - a_5 \sinh \delta_m) + \Delta_{160}, \\ \Delta_{160} &= \frac{2\delta_m E_{2m}}{(\delta_m^2 - a_m^2)^2} (a_5 \cosh \delta_m - a_4 \sinh \delta_m) \\ \Delta_{17} &= \widehat{T} \cosh a, \Delta_{18} = \frac{a_m \sinh a}{a}, \\ \Delta_{19} &= \Delta_9 - (\Delta_{10} - \Delta_{11}) \cosh a - \frac{(\Delta_{12} - \Delta_{13}) \sinh a}{a} \end{aligned}$$

From the boundary condition (29), we have

$$M = \frac{-D^2 W(1)}{a^2 \theta(1)}$$

The thermal Marangoni number for a linear temperature profile is as follows

$$M_1 = -\frac{[\delta^2 (\cosh \delta + a_1 \sinh \delta) + \zeta^2 (a_2 \cosh \zeta + a_3 \sinh \zeta)]}{a^2 (c_1 \cosh a + c_2 \sinh a + \Lambda_1 + \Lambda_2)} \tag{35}$$

where

$$\begin{aligned} \Lambda_1 &= \frac{(E_2 + E_1)}{(\delta^2 - a^2)} (\cosh \delta + a_1 \sinh \delta) - \frac{2\delta E_2}{(\delta^2 - a^2)^2} (a_1 \cosh \delta + \sinh \delta) \\ \Lambda_2 &= \frac{(E_2 + E_1)}{(\zeta^2 - a^2)} (a_2 \cosh \zeta + a_3 \sinh \zeta) - \frac{2\zeta E_2}{(\zeta^2 - a^2)^2} (a_3 \cosh \zeta + a_2 \sinh \zeta) \end{aligned}$$

4.2. Parabolic temperature profile. For the parabolic temperature profile

$$h(z) = 2z \quad \text{and} \quad h_m(z_m) = 2z_m \tag{36}$$

Substituting (36) into (26) and (28), the temperature distributions θ and θ_m are obtained using the temperature boundary conditions is as follows

$$\theta(z) = A_1 [c_5 \cosh az + c_6 \sinh az + g_2(z)] \tag{37}$$

$$\theta_m(z_m) = A_1 [c_7 \cosh a_m z_m + c_8 \sinh a_m z_m + g_{m2}(z_m)] \tag{38}$$

where

$$\begin{aligned} g_2(z) &= A_1 [\delta_{11} - \delta_{12} + \delta_{13} - \delta_{14}], g_{m2}(z_m) = A_1 [\delta_{15} - \delta_{16}] \\ \delta_{11} &= \frac{(E_4 z + E_3)}{(\delta^2 - a^2)} (\cosh \delta z + a_1 \sinh \delta z) \\ \delta_{12} &= \frac{2\delta E_4}{(\delta^2 - a^2)^2} (a_1 \cosh \delta z + \sinh \delta z) \end{aligned}$$

$$\begin{aligned} \delta_{13} &= \frac{(E_4 z + E_3)}{(\zeta^2 - a^2)}(a_2 \cosh \zeta z + a_3 \sinh \zeta z) \\ \delta_{14} &= \frac{2\zeta E_4}{(\zeta^2 - a^2)^2}(a_3 \cosh \zeta z + a_2 \sinh \zeta z) \\ \delta_{15} &= \frac{(E_{3m} + E_{4m} z_m)}{(\delta_m^2 - a_m^2)}(a_4 \cosh \delta_m z_m + a_5 \sinh \delta_m z_m) \\ \delta_{16} &= \frac{2E_{4m} \delta_m}{(\delta_m^2 - a_m^2)^2}(a_5 \cosh \delta_m z_m + a_4 \sinh \delta_m z_m), \\ E_3 &= R_I^*, E_4 = -2(R_I^* + 1), E_{3m} = -R_{Im}^*, E_{4m} = -2(R_{Im}^* + 1) \\ c_5 &= c_7 \hat{T} + \Delta_{21} - \Delta_{22}, c_6 = \frac{1}{a}(c_8 a_m + \Delta_{23} - \Delta_{24}), \\ c_7 &= \frac{\Delta_{27} \Delta_{29} + \Delta_{30} \Delta_{26}}{\Delta_{25} \Delta_{29} + \Delta_{26} \Delta_{28}}, c_8 = \frac{\Delta_{27} \Delta_{28} - \Delta_{25} \Delta_{29}}{-\Delta_{26} \Delta_{28} - \Delta_{25} \Delta_{29}}, \\ \Delta_{20} &= -[\delta_{17} - \delta_{18} + \delta_{19} - \delta_{20}], \\ \delta_{17} &= \frac{(E_4 + E_3)}{(\delta^2 - a^2)}(\cosh \delta + a_1 \sinh \delta), \\ \delta_{18} &= \left[\frac{2\delta E_4}{(\delta^2 - a^2)^2} \right] (a_1 \cosh \delta + \sinh \delta), \\ \delta_{19} &= \frac{(E_4 + E_3)}{(\zeta^2 - a^2)}(a_2 \cosh \zeta + a_3 \sinh \zeta), \\ \delta_{20} &= \left[\frac{2\zeta E_4}{(\zeta^2 - a^2)^2} \right] (a_3 \cosh \zeta + a_2 \sinh \zeta), \\ \Delta_{21} &= \hat{T} \left[\frac{E_{3m} a_4}{(\delta_m^2 - a_m^2)} - \frac{2E_{4m} \delta_m a_5}{(\delta_m^2 - a_m^2)^2} \right], \\ \Delta_{22} &= \frac{E_3}{(\delta^2 - a^2)} - \frac{2\delta a_1 E_4}{(\delta^2 - a^2)^2} + \frac{a_2 E_3}{(\zeta^2 - a^2)} - \frac{2\zeta a_3 E_4}{(\zeta^2 - a^2)^2}, \\ \Delta_{23} &= \left[\frac{E_{4m}}{(\delta_m^2 - a_m^2)} - \frac{2\delta_m^2 E_{4m}}{(\delta_m^2 - a_m^2)^2} \right] a_4 + \frac{a_5 E_{3m}}{(\delta_m^2 - a_m^2)} \\ \Delta_{24} &= \frac{E_3 \delta a_1 + E_4}{(\delta^2 - a^2)} - \frac{2E_4 \delta^2}{(\delta^2 - a^2)^2} + \frac{E_3 \zeta a_3 + E_4 a_2}{(\zeta^2 - a^2)} - \frac{2a_2 E_4 \zeta^2}{(\zeta^2 - a^2)^2}, \\ \Delta_{25} &= \cosh a_m, \Delta_{26} = \sinh a_m, \\ \Delta_{27} &= -\frac{E_{3m} - E_{4m}}{(\delta_m^2 - a_m^2)}(a_4 \cosh \delta_m - a_5 \sinh \delta_m) + \Delta_{270}, \\ \Delta_{270} &= \frac{2\delta_m E_{4m}}{(\delta_m^2 - a_m^2)^2}(a_5 \cosh \delta_m - a_4 \sinh \delta_m), \\ \Delta_{28} &= \hat{T} \cosh a, \Delta_{29} = \frac{a_m \sinh a}{a}, \\ \Delta_{30} &= \Delta_{20} - (\Delta_{21} - \Delta_{22}) \cosh a - \frac{(\Delta_{23} - \Delta_{24}) \sinh a}{a} \end{aligned}$$

From the boundary condition (29), the thermal Marangoni number for a parabolic temperature profile is as follows

$$M_2 = -\frac{[\delta^2(\cosh \delta + a_1 \sinh \delta) + \zeta^2(a_2 \cosh \zeta + a_3 \sinh \zeta)]}{a^2(c_5 \cosh a + c_6 \sinh a + \Lambda_3 + \Lambda_4)} \tag{39}$$

where

$$\begin{aligned} \Lambda_3 &= \frac{(E_4 + E_3)}{(\delta^2 - a^2)}(\cosh \delta + a_1 \sinh \delta) - \frac{2\delta E_4}{(\delta^2 - a^2)^2}(a_1 \cosh \delta + \sinh \delta) \\ \Lambda_4 &= \frac{(E_4 + E_3)}{(\zeta^2 - a^2)}(a_2 \cosh \zeta + a_3 \sinh \zeta) - \frac{2\zeta E_4}{(\zeta^2 - a^2)^2}(a_3 \cosh \zeta + a_2 \sinh \zeta) \end{aligned}$$

4.3. Inverted Parabolic temperature profile. Consider this profile

$$h(z) = 2(1 - z) \quad \text{and} \quad h_m(z_m) = 2(1 - z_m) \quad (40)$$

Substituting (40) into (26) and (28), the temperature distributions θ and θ_m are obtained using the temperature boundary conditions, as follows

$$\theta(z) = A_1[c_9 \cosh az + c_{10} \sinh az + g_3(z)] \quad (41)$$

$$\theta_m(z_m) = A_1[c_{11} \cosh a_m z_m + c_{12} \sinh a_m z_m + g_{m3}(z_m)] \quad (42)$$

where

$$g_3(z) = A_1[\delta_{21} - \delta_{22} + \delta_{23} - \delta_{24}], \quad g_{m3}(z_m) = A_1[\delta_{25} - \delta_{26}]$$

$$\delta_{21} = \frac{(E_6 z + E_5)}{(\delta^2 - a^2)} (\cosh \delta z + a_1 \sinh \delta z)$$

$$\delta_{22} = \frac{2\delta E_6}{(\delta^2 - a^2)^2} (a_1 \cosh \delta z + \sinh \delta z)$$

$$\delta_{23} = \frac{(E_6 z + E_5)}{(\zeta^2 - a^2)} (a_2 \cosh \zeta z + a_3 \sinh \zeta z)$$

$$\delta_{24} = \frac{2\zeta E_6}{(\zeta^2 - a^2)^2} (a_3 \cosh \zeta z + a_2 \sinh \zeta z)$$

$$\delta_{25} = \frac{(E_{5m} + E_{6m} z_m)}{(\delta_m^2 - a_m^2)} (a_4 \cosh \delta_m z_m + a_5 \sinh \delta_m z_m)$$

$$\delta_{26} = \frac{2E_{6m} \delta_m}{(\delta_m^2 - a_m^2)^2} (a_5 \cosh \delta_m z_m + a_4 \sinh \delta_m z_m),$$

$$E_5 = R_I^* - 2, E_6 = 2(1 - R_I^*), E_{5m} = -2 - R_{Im}^*, E_{6m} = 2(1 - R_{Im}^*)$$

$$c_9 = c_{11} \hat{T} + \Delta_{32} - \Delta_{33}, \quad c_{10} = \frac{1}{a} (c_{12} a_m + \Delta_{34} - \Delta_{35}),$$

$$c_{11} = \frac{\Delta_{38} \Delta_{40} + \Delta_{37} \Delta_{41}}{\Delta_{40} \Delta_{36} + \Delta_{37} \Delta_{39}}, \quad c_{12} = \frac{\Delta_{38} \Delta_{39} - \Delta_{36} \Delta_{41}}{-\Delta_{39} \Delta_{37} - \Delta_{36} \Delta_{40}},$$

$$\Delta_{31} = -[\delta_{27} - \delta_{28} + \delta_{29} - \delta_{30}],$$

$$\delta_{27} = \frac{(E_6 + E_5)}{(\delta^2 - a^2)} (\cosh \delta + a_1 \sinh \delta),$$

$$\delta_{28} = \left[\frac{2\delta E_6}{(\delta^2 - a^2)^2} \right] (a_1 \cosh \delta + \sinh \delta),$$

$$\delta_{29} = \frac{(E_6 + E_5)}{(\zeta^2 - a^2)} (a_2 \cosh \zeta + a_3 \sinh \zeta),$$

$$\delta_{30} = \left[\frac{2\zeta E_6}{(\zeta^2 - a^2)^2} \right] (a_3 \cosh \zeta + a_2 \sinh \zeta),$$

$$\Delta_{32} = \hat{T} \left[\frac{E_{5m} a_4}{(\delta_m^2 - a_m^2)} - \frac{2E_{6m} \delta_m a_5}{(\delta_m^2 - a_m^2)^2} \right],$$

$$\Delta_{33} = \frac{E_5}{(\delta^2 - a^2)} - \frac{2\delta a_1 E_6}{(\delta^2 - a^2)^2} + \frac{a_2 E_5}{(\zeta^2 - a^2)} - \frac{2\zeta a_3 E_6}{(\zeta^2 - a^2)^2},$$

$$\Delta_{34} = \left[\frac{E_{6m}}{(\delta_m^2 - a_m^2)} - \frac{2\delta_m^2 E_{6m}}{(\delta_m^2 - a_m^2)^2} \right] a_4 + \frac{a_5 E_{5m}}{(\delta_m^2 - a_m^2)}$$

$$\Delta_{35} = \frac{E_5 \delta a_1 + E_6}{(\delta^2 - a^2)} - \frac{2E_6 \delta^2}{(\delta^2 - a^2)^2} + \frac{E_5 \zeta a_3 + E_6 a_2}{(\zeta^2 - a^2)} - \frac{2a_2 E_6 \zeta^2}{(\zeta^2 - a^2)^2},$$

$$\Delta_{36} = \cosh a_m, \quad \Delta_{37} = \sinh a_m,$$

$$\Delta_{38} = -\frac{E_{5m} - E_{6m}}{(\delta_m^2 - a_m^2)} (a_4 \cosh \delta_m - a_5 \sinh \delta_m) + \Delta_{380},$$

$$\Delta_{380} = \frac{2\delta_m E_{6m}}{(\delta_m^2 - a_m^2)^2} (a_5 \cosh \delta_m - a_4 \sinh \delta_m),$$

$$\Delta_{39} = \hat{T} \cosh a, \Delta_{40} = \frac{a_m \sinh a}{a},$$

$$\Delta_{41} = \Delta_{31} - (\Delta_{32} - \Delta_{33}) \cosh a - \frac{(\Delta_{34} - \Delta_{35}) \sinh a}{a}$$

From the boundary condition (29), the thermal Marangoni number for a inverted parabolic temperature profile is as follows

$$M_3 = -\frac{[\delta^2(\cosh \delta + a_1 \sinh \delta) + \zeta^2(a_2 \cosh \zeta + a_3 \sinh \zeta)]}{a^2(c_9 \cosh a + c_{10} \sinh a + \Lambda_5 + \Lambda_6)} \tag{43}$$

where

$$\Lambda_5 = \frac{(E_6 + E_5)}{(\delta^2 - a^2)}(\cosh \delta + a_1 \sinh \delta) - \frac{2\delta E_6}{(\delta^2 - a^2)^2}(a_1 \cosh \delta + \sinh \delta)$$

$$\Lambda_6 = \frac{(E_6 + E_5)}{(\zeta^2 - a^2)}(a_2 \cosh \zeta + a_3 \sinh \zeta) - \frac{2\zeta E_6}{(\zeta^2 - a^2)^2}(a_3 \cosh \zeta + a_2 \sinh \zeta)$$

5. RESULTS AND DISCUSSION

The thermal Marangoni numbers M_1 for linear, M_2 for parabolic and M_3 for inverted parabolic temperature profiles which are the Eigen values are obtained as an expression of the horizontal wavenumbers a and a_m , the Chandrasekhar number Q , the porous parameter β , the thermal ratio \hat{T} , the modified internal Rayleigh numbers R_I^* and R_{Im}^* for the fluid and porous layers respectively and the depth ratio \hat{d} . These Marangoni numbers are drawn as a function of depth ratio using Mathematica software. From the graphs it is clear that, for lower values of depth ratios, there is no much change in the thermal Marangoni numbers and increases for further increase in the values of the depth ratio. The effects of the parameters a , β , Q , R_I^* and \hat{T} on the thermal Marangoni numbers M_1, M_2 and M_3 are shown in the following figures for linear, Parabolic and inverted parabolic temperature profiles for fixed values of $Q = 50, \varepsilon = 1, \beta = 0.1, a = 1.0, \hat{T} = 1.5, R_I^* = -3$ and $R_{Im}^* = 1$.

The effects of the horizontal wavenumber a on the thermal Marangoni number is exhibited in the figures 2a,2b and 2c for linear, parabolic and inverted parabolic temperature profiles respectively and they are for $a = 0.9, 1.0$ and 1.1 . The effects of a are analogous for all the three profiles and for a fixed value of depth ratio, the increase in the value of the horizontal wavenumber for the fluid layer a , decreases the value of the thermal Marangoni number. That is the Magneto-Marangoni convection sets in earlier favoring the situations of demanding convection. Hence the increase in the value of a destabilizes the system which is conducive for the situations which require convection namely heat transfer problems.

The effects of the porous parameter β on the thermal Marangoni number are displayed in the figures 3a,3b and 3c respectively for linear, parabolic and inverted parabolic temperature profiles for $\beta = 0.1, 0.2$ and 0.3 . The effects of β are similar for all the three profiles and for a fixed value of depth ratio, the increase in the value of the porous parameter β , increases the value of the thermal Marangoni number. That is the Magneto-Marangoni convection is delayed. Hence the increase in the value of β stabilizes the system which is conducive for the situations where in the convection is to be controlled. Also the diverging curves indicate that the effect of the porous parameter is drastic for the larger values of depth ratios, hence this parameter plays an important role in the porous layer dominant composite systems.

The effects of the Chandrasekhar number Q on the thermal Marangoni numbers is depicted in figures 4a, 4b and 4c for linear, parabolic and inverted parabolic temperature profiles respectively and they are for $Q = 50, 60$ and 70 . The effects of Q is same for

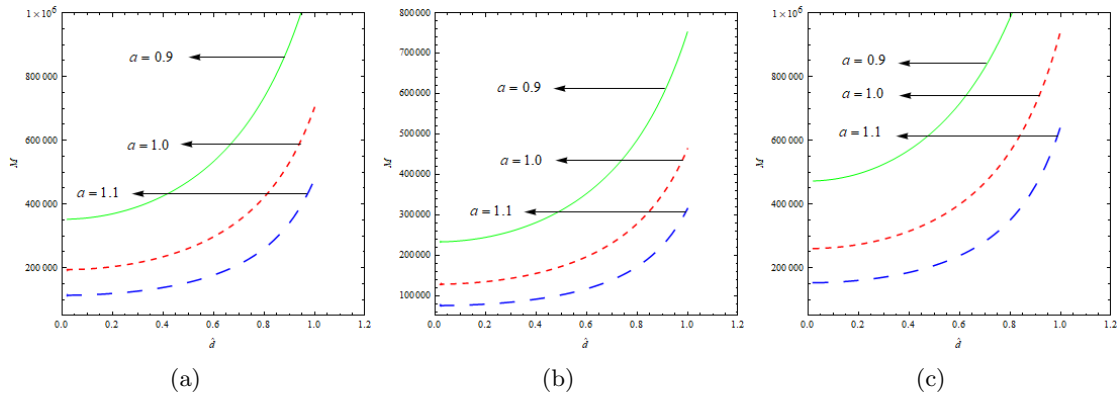


FIGURE 2. M versus \hat{d} for different values of horizontal wave number a

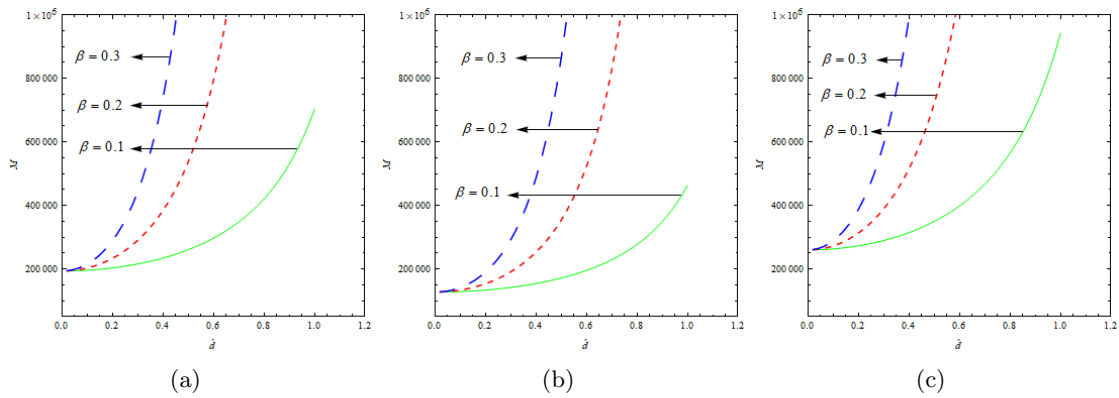


FIGURE 3. M versus \hat{d} for different values of porous parameter β

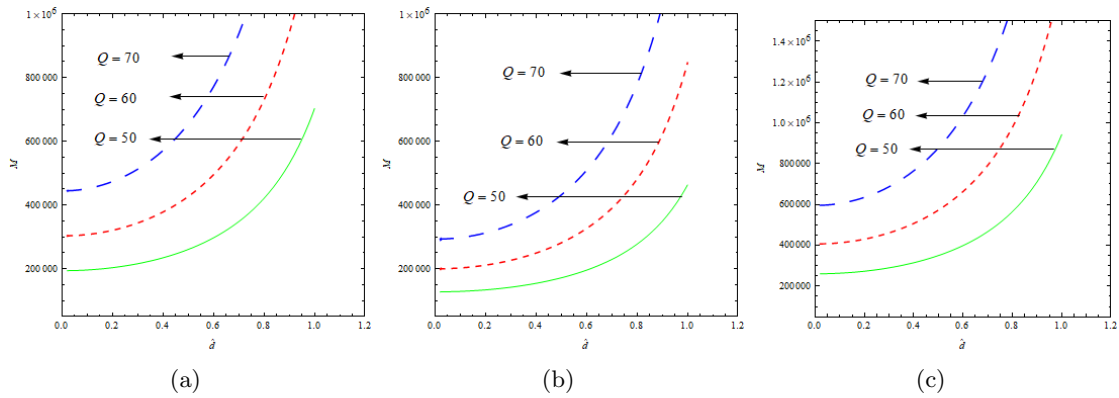


FIGURE 4. M versus \hat{d} for different values of Chandrasekhar number Q

all the three profiles and for a fixed value of depth ratio, the increase in the value of Chandrasekhar number Q , increases the value of the thermal Marangoni number. That is the Magneto-Marangoni convection is delayed. Hence the presence of a magnetic field stabilizes the system.

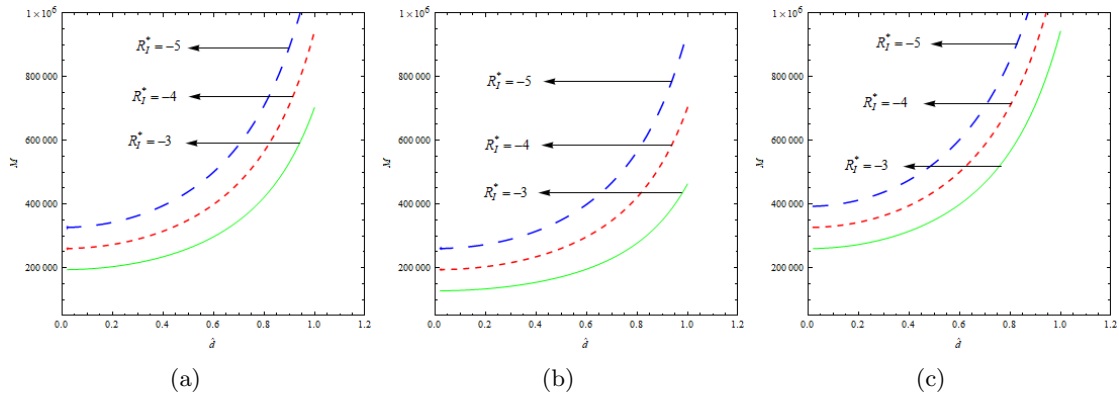


FIGURE 5. M versus \hat{d} for different values of modified internal Rayleigh number R_I^*

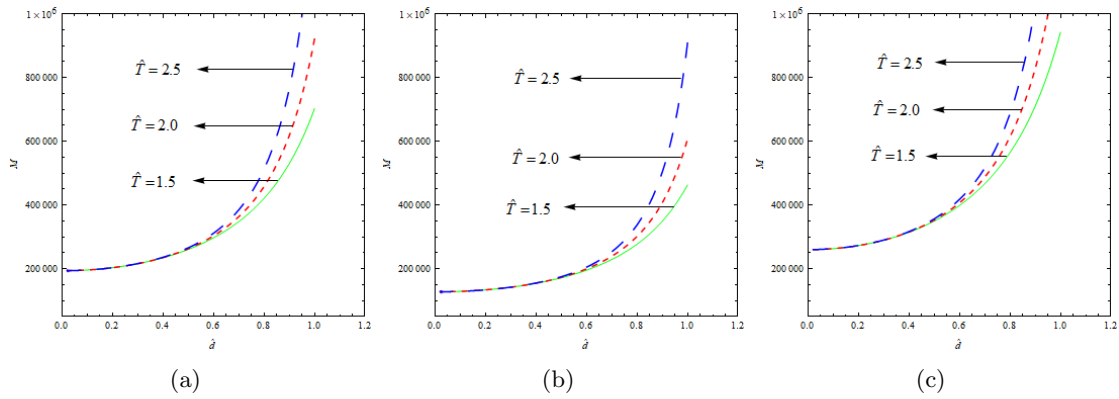


FIGURE 6. M versus \hat{d} for different values of thermal ratio \hat{T}

The effect of modified internal Rayleigh number R_I^* on the Marangoni number is similar for all the three temperature profiles depicted the figures 5a, 5b, 5c for $R_I^* = -3, -4$ and -5 . Decreasing the values of R_I^* , the Marangoni number increases, which is physically reasonable as the absorption of heat stabilizes the system, hence the Magneto-Marangoni convection can be delayed by decreasing the values of R_I^* . The effects of the thermal ratio \hat{T} on the thermal Marangoni numbers is presented in figures 6a, 6b and 6c for linear, parabolic and inverted parabolic temperature profiles respectively and they are for $\hat{T} = 1.5, 2.0$ and 2.5 . The effects of \hat{T} is the same for all the three profiles and for a fixed value of depth ratio, the increase in the value of thermal ratio \hat{T} , increases the value of the thermal Marangoni number. That is the Magneto-Marangoni convection is delayed. Hence the system is stabilized. Since the curves are slightly diverging, the effect of this ratio is prominent for larger values of depth ratios.

6. CONCLUSIONS

Text of the conclusion Following conclusions are drawn from this study

- (i) The effects of the physical parameters is qualitatively similar for both uniform and nonuniform temperature gradients considered in the study.

- (ii) The inverted parabolic profile is the highly stable of all the three temperature gradients.
- (iii) By declining the values of the horizontal wave number a and the modified internal Rayleigh number R_I^* , one can postpone the Darcy-Bènard-Magneto-Marangoni convection. Hence these two parameters play an important role to control convection in the manufacture of crystals.
- (iv) By lessening the values of porous parameter β , the Chandrasekhar number Q and the thermal ratio \hat{T} , Darcy-Bènard-Magneto-Marangoni convection can be preponed.
- (v) There is no effect of modified internal Rayleigh number R_{Im}^* for porous layer on the Darcy-Bènard-Magneto-Marangoni convection.
- (vi) The parameters β , Q and \hat{T} play an important role in the porous layer dominant composite layer.
- (vii) Smaller values of horizontal wave number, modified internal Rayleigh number and larger values of porous parameter, Chandrasekhar number and thermal ratio can be utilized to control convection in the manufacture of crystals. So, this study is very much useful for crystal growth industries.

Acknowledgement. Authors acknowledge the support from REVA University for the facilities provided to carry out the research and also they are thankful to Late Prof. N. Rudraiah and Hon. Prof. I. S. Shivakumara, (Department of Mathematics, Bangalore University, Bengaluru) for their help during the formulation of the problem. The authors would like to thank the reviewer(s) for their useful comments that helped us to improve this paper.

REFERENCES

- [1] Sankar, M., Venkatachalappa, M., and Shivakumara, I.S., (2006), Effect of magnetic field on natural convection in a vertical cylindrical annulus, *International Journal of Engineering Science*, 44(20), pp. 1556-1570.
- [2] Sankar, M., YoungyongPark., Lopez, J.M., and YounghaeDo., (2011), Numerical study of natural convection in a vertical porous annulus with discrete heating, *International Journal of Heat and Mass Transfer*, 54(7-8), pp. 1493-1505.
- [3] Sankar, M., Junpyo Park., Dongseok Kim, & Younghae Do., (2013) Numerical study of natural convection in a vertical porous annulus with an internal heat source: Effect of discrete heating, *Numerical Heat Transfer, Part A: Applications*, 63(9), pp. 687-712.
- [4] Swati Mukhopadhyay., (2008), Natural convection flow on a sphere through porous medium in presence of heat source/sink near a stagnation point, *Mathematical Modelling and Analysis*, 13(4), pp.513-520.
- [5] Umavathi, J.C., Prathap Kumar, and Jaweriya Sultana., (2012), Mixed convection flow in vertical channel with boundary conditions of third kind in presence of heat source/sink, *Appl. Math. Mech. Engl. Ed.*, 33(8), pp. 1015-1034.
- [6] Brian Straughan, (2014), Resonant penetrative convection with an internal heat source/sink, *Acta Applicandae Mathematicae*, 132(1), pp. 561-581.
- [7] Thomas Mwathi Ngugi, Mathew Ngugi Kinyanjui, and David Theuri., (2016), Effects of mass transfer on unsteady hydromagnetic convective flow past an infinite vertical rotating porous plate with heat source, *American Journal of Applied Mathematics*, 4(3), pp. 114-123.
- [8] Malvandi, A., Moshizi, S.A., and Ganji, D.D., (2016), Nanofluids flow in microchannels in presence of heat source/sink and asymmetric heating, *Journal of Thermo physics and Heat Transfer*, 30(1), pp. 111-119.
- [9] Baag, S., Mishra, S. R., and Samantray, B.L., (2017), Buoyancy effects on free convective MHD flow in the presence of heat source/sink, *AMSE Journals, AMSE IIETA publication- 2017 Series: Modelling B*; 86(1), pp. 14-32.
- [10] Umavathi, J.C., Prathap Kumar, Ioan Pop, and Shekar Marudappa., (2017), Flow and heat transfer of couple stress fluid in a vertical channel in the presence of heat source/sink, *International Journal of Numerical Methods for Heat and Fluid Flow*, 27(4), pp. 1-32.

- [11] Arun Kumar Singh, and Ashok Kumar Singh., (2017), Effect of heat source/sink on free convective flow of a polar fluid between vertical concentric annuli, *Journal of Applied Mathematics and Physics*, 5, 1750-1762.
- [12] Ganesh Kumar, K., Gireesha, B.J., Krishnamurthy, M. R. and Prasannakumara, B.C., (2018), Impact of convective condition on Marangoni convection flow and heat transfer in Casson-Nanofluid with uniform heat source sink, *Journal of Nanofluids*, 7(1), pp. 108-114.
- [13] Anjali Devi, S.P., Agneeshwari, M. and Wilfred Samuel Raj, J., (2018), Radiation effects on MHD boundary layer flow and heat transfer over a nonlinear stretching surface with variable wall temperature in the presence of non-uniform heat source/sink, *Int. J. of Applied Mechanics and Engineering*, 23 (2), pp. 289-305.
- [14] Ramachandramurthy, V. and Aruna, A.S., (2018), Rayleigh-Bènard-Taylor convection in temperature-sensitive Newtonian liquid with heat source/sink, *International Journal of Engineering Research & Technology* , 7 (7), pp. 166-170.
- [15] Garg, B.P., and Shipra., (2018), Effect of heat source/sink on free connective MHD flow past an exponentially accelerated infinite plate with mass diffusion and chemical reaction, *Journal of Rajasthan Academy of Physical Sciences*, 17(3&4) pp. 151-164.
- [16] Garg, B.P., and Shipra., (2019), Exact solution of MHD free convective and mass transfer flow near a moving vertical plate in the presence of heat source/sink, *Journal of Rajasthan Academy of Physical Sciences*, 18 (1&2), pp. 25-44.
- [17] Garg, B.P., and Shipra., (2019), Effect of heat source/sink on unsteady free convective MHD flow past a linearly accelerated vertical plate with mass diffusion, *International Journal of Scientific Research and Reviews*, 8 (2), pp. 1437-1454.
- [18] Shipra, and Garg, B.P., (2019), Effect of heat source/sink on free connective MHD flow past an exponentially accelerated infinite plate with mass diffusion and chemical reaction, *International Journal of Innovative Technology and Exploring Engineering*, 8 (9S), pp. 696-702.
- [19] Girish, N., Sankar, M., & Keerthi Reddy., (2019), Analysis of fully developed mixed convection in open-ended annuli with viscous dissipation, *J. Therm. Anal. Calorim.*, <https://doi.org/10.1007/s10973-019-09120-9>.
- [20] Girish N., Sankar, M., and O. D. Makinde., (2020), Developing Buoyant convection in vertical porous annuli with unheated entry and exit, *Heat Transfer-Asian Res.*, 49(5), pp. 2551-2576.
- [21] Naveen Dwivedi, and Ashok kumar Singh., (2020), Influence of Hall current on hydromagnetic natural convective flow between two vertical concentric cylinders in presence of heat source/sink, *Heat Transfer-Asian Res.*, 49 (3), pp. 1402-1417.
- [22] Mebarek-Oudina, F., Keerthi Reddy, N., Sankar, M., (2021) Heat source location effects on Buoyant convection of nanofluids in an annulus. In: Rushi Kumar B., Sivaraj R., Prakash J. (eds), *Advances in Fluid Dynamics. Lecture Notes in Mechanical Engineering*, Springer, Singapore. https://doi.org/10.1007/978-981-15-4308-1_70.
- [23] Sumithra, R., and Manjunatha, N., (2012), Analytical study of surface tension driven magneto convection in a composite layer bounded by adiabatic boundaries, *International Journal of Engineering and Innovative Technology*, 6 (1), pp. 249-257.
- [24] Sumithra, R., and Manjunatha, N., (2014), Effects of parabolic and inverted parabolic temperature gradients on magneto Marangoni convection in a composite layer, *International Journal of Current Research*, 6 (3), pp. 5435-5450.
- [25] Sumithra, R., and Manjunatha, N., (2020), Effects of heat source/sink and non uniform temperature gradients on Darcian-Bènard-Magneto-Marangoni convection in composite layer horizontally enclosed by adiabatic boundaries, *Malaya Journal of Matematik*, 8(2), pp. 373-382.
- [26] Sumithra, R., Manjunatha, N., and Komala, B., (2020), Effects of heat source/sink and non-uniform temperature gradients on non-Darcian-Bènard-Magneto-Marangoni convection in an infinite horizontal composite layer, *International journal of Applied Engineering Research*, 15(6), pp. 600-608.



Manjunatha N. received his M.Sc., Mathematics degree in 2004 from Bangalore University, Bangalore, and M.Phil., Mathematics degree from Alagappa University, Tamilnadu in 2008, and Ph.D. Mathematics degree from Bharathiar University, Tamilnadu in 2019. Currently, he is working as an associate professor in the Department of Mathematics, School of Applied Sciences, REVA University, Bengaluru, India. His area of research is Fluid Mechanics and Heat & Mass transfer.



Sumithra R. was awarded her M.Phil. degree in 1994 and Ph.D. in Mathematics in the year 2000. Her specialization is Fluid Mechanics and Magneto hydrodynamics. Currently, she is working as an associate professor and head of the Department of UG, PG Studies & Research in Mathematics, Nrupathunga University, Bengaluru, Karnataka, India.
